Cross Section Limits for the Formation of $^{266}107$ in the ^{254}Es + ^{16}O Reaction

M. Schädel, W. Brüchle, E. Jäger, K. Sümmerer
GSI Darmstadt
E.K. Hulet, J.F. Wild, R.W. Lougheed, R. J. Dougan, K.J. Moody
LLNL Livermore, CA

In a previous contribution we have reported on experimental details[1], measured α-spectra, and also on the chemical separation[2] of an element 107 fraction from the irradiation of a 49 μg/cm^2 ^{254}Es target with 93 MeV and 96 MeV ^{16}O ions. This search for evaporation residues in the $^{254}Es(^{16}O,4n)^{266}107$ reaction was motivated by theoretical calculations of fission barriers and nuclear masses[3,4,5] and the comparison of these results with experimental data[6]. From these results one can conclude that nuclides in a region of enhanced nuclear stability around Z = 110 and N = 162 may have half-lives long enough that their decay can be observed in radiochemical experiments.
In a first analysis[1] all α-events below an energy of 7.5 MeV were assigned to small amounts of Fm and Md isotopes. From the sum of all experiments (93 MeV and 96 MeV projectile energy, 5s and 30s cycle time of the rotating wheel) we obtained 21 α-events between 8.5 MeV and 9.1 MeV, see Fig. 1.

An assignment to known isotopes can be made for all events below 8.95 MeV. However, one has to note that in many cases this is not a unique assignment and that some ambiguities are left. The following assignments have been made:

(1) The group at 8.90 MeV originates from Po-211m. An assignment to $^{261}105$ can be excluded as long as there is no indication for the existence of a longer-lived precursor ($T_{1/2} \geq 20s$).

(2) The α-events between 8.72 and 8.82 MeV belong to Po-212 as a daughter of Bi-212. An assignment to $^{259}104$ and ^{257}Lr can be excluded because of their half-lives being too short and no precursors with sufficiently long half-lives are known.

(3) Possible candidates for the region between 8.52 and 8.69 MeV are $^{256,258}Lr$ and $^{262}105$ except that there are the following inconsistencies with such an assignment. No α-event has been observed at 8.45 MeV where the most intense α-line with an abundance of 75% is expected for $^{262}105$,and because of the short half-life ^{258}Lr can only be observed as a daughter of the longer-lived $^{262}105$. An assignment of the events at 8.52 Mev to Po-212m is unlikely because only 2% relative intensity is expected to be found in this transition compared with 97% at 11.6 MeV which was not observed in the experiment.

Most interesting are four events above 8.95 MeV. All of them appeared in experiments with 30s cycle time, three events in the first and second detector at 93 MeV ^{16}O projectile energy, and the one event at 9.04 MeV at detector number seven in an irradiation with 96 MeV ^{16}O projectile energy. The asssignment of the 9.08 MeV alpha to Po-212m can be excluded, see above. A remaining candidate for the three events observed at 93 MeV bombarding energy may be the isotope $^{257}104$, which again is not very likely because only production mechanisms with low cross sections like a multinucleon transfer from ^{254}Es or a $^{250}Cf(^{16}O,5n)^{261}106$ reaction followed by α-decay to $^{257}104$ can lead to this isotope and because of the depletion of element 104 products by the chemical separation. We have to conclude that the four α-events at about 9.04 MeV remain unassigned. Because of the absence of the observation of any correlated, successive α-decays into the region of known nuclei (mother-daughter correlations) we are not able to assign any event to the isotope $^{266}107$. We have used the four events above 8.95 MeV to calculate upper limit cross sections. The result with a 95% confidence level is shown in Fig.2 as a function of the half-life assumed. The two curves correspond to two extreme limits in the assumption about the transport time from the target to the detection system.

1. M. Schädel et al., GSI 87-1, 1987, p. 15
2. E. Jäger, M. Schädel, GSI 87-1, 1987, p. 255
3. P. Moller et al., Z. Phys. A323, 41 (1986)
4. S. Cwiok et al., Nucl. Phys. A444, 1 (1985)
5. K. Böning et al., Z. Phys. A325, 479 (1986)
6. G. Münzenberg et al., Z. Phys. A328, 49 (1987)

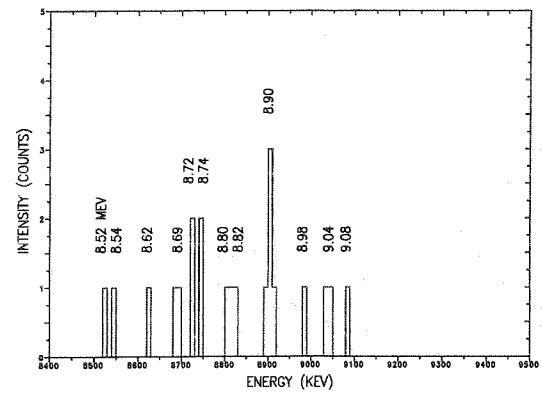

Fig.1: Sum of all α-spectra between 8.4 and 9.5 MeV from all experiments at 93 MeV and 96 MeV ^{16}O on ^{254}Es.

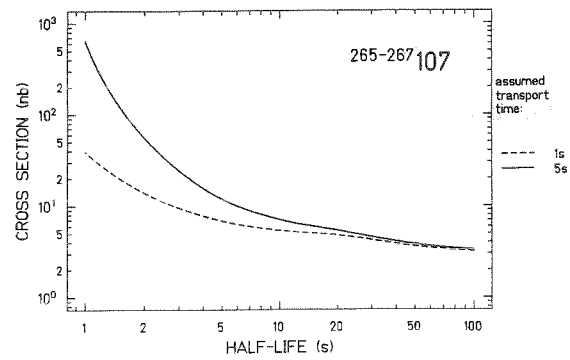

Fig.2: Upper-limit cross sections for the production of $^{266}107$ (95% conf. level) as a function of an assumed half-life.

Nucleon Transfer in the Fusion Hindered System Sn + Zr

R.Bellwied, J.V.Kratz
Institut für Kernchemie der Universität Mainz
W.Reisdorf, D.Schüll
GSI Darmstadt
B.Kohlmeyer
Universität Marburg
R.Künkel
HMI Berlin

To continue our general studies of the competition between direct reactions with fusion /1,2/, we measured mass, charge, and energy distributions in the systems $^{96}Zr + {}^{90}Zr$ and $^{124}Sn + {}^{96}Zr$ near the Coulomb barrier at the GSI magnetic spectrometer. The 1987 experiments using 4.15 MeV/u ^{96}Zr, ^{124}Sn beams from the UNILAC complement earlier measurements in the system $^{90}Zr + {}^{96}Zr$ /1/. We carried out measurements from $\Theta_{lab} = 5^{\circ}$ to 40° in steps of 5°. Experimental difficulties that arose in the 1985 run were overcome by using a thinner scintillator foil in the focal plane of the spectrometer and by using inverse kinematics, resulting in an improved energy and Z resolution in the ionisation chamber.

Figs.1,2 show mass and charge distributions for transfer products around the target in the $^{124}Sn + {}^{96}Zr$ system. At 25° (lab) masses from A = 90 up to A = 100 can be well resolved. The distribution spreads over a wider range than that in the Zr + Zr case /1/.

The Z-distribution in Fig.2 is determined by the analysis of the ΔE-E signals. We show an integrated Z spectrum that is also broadened compared to the Zr + Zr system (inside histogram). Relative cross sections as a function of Z and A are shown in Fig.3. From a look at the various panels it is obvious that the largest cross sections are one- and two-neutron pick-up as well as stripping reactions. Charged particle transfer is not negligible however and accounts exclusively for the yields at masses lighter than A = 94 up to a dominant α-transfer in the A = 92 bin.

These results show in comparison to the Zr + Zr system /1/, that there are far more open transfer channels in the heavier system where fusion is hindered. It will be interesting to test critically whether this observed dramatic increase in the transfer cross sections is indeed correlated with the similarly striking onset of the 'extra-push' phenomenon /3/, observed earlier in this region of entrance channel fissility /4/. This correlation had already been suggested from a systematic study of transfer cross sections between systems in the vicinity of the 'extra-push' threshold at fusion barrier energies /2/.

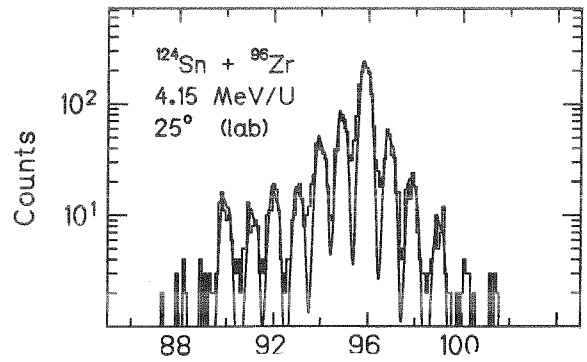

Fig.1: Mass distribution

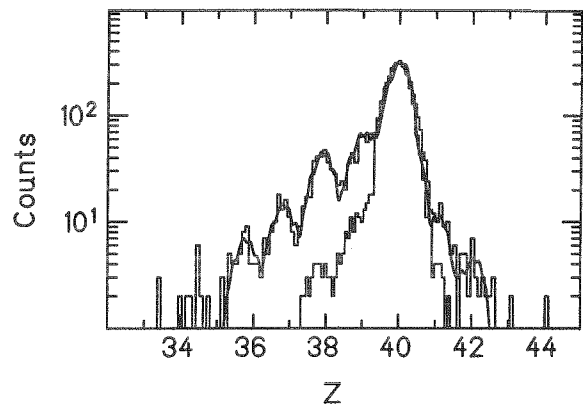

Fig.2: Charge distributions for the $^{124}Sn + {}^{96}Zr$ system at 4.15 MeV/u at $\Theta_{lab} = 25^{\circ}$ (main histogram) and the $^{96}Zr + {}^{90}Zr$ system at 4.15 MeV/u at $\Theta_{lab} = 35^{\circ}$ (inside histogram). At these angles the nucleon exchange is dominant. The Zr+Zr curve is normalized to the Sn+Zr curve.

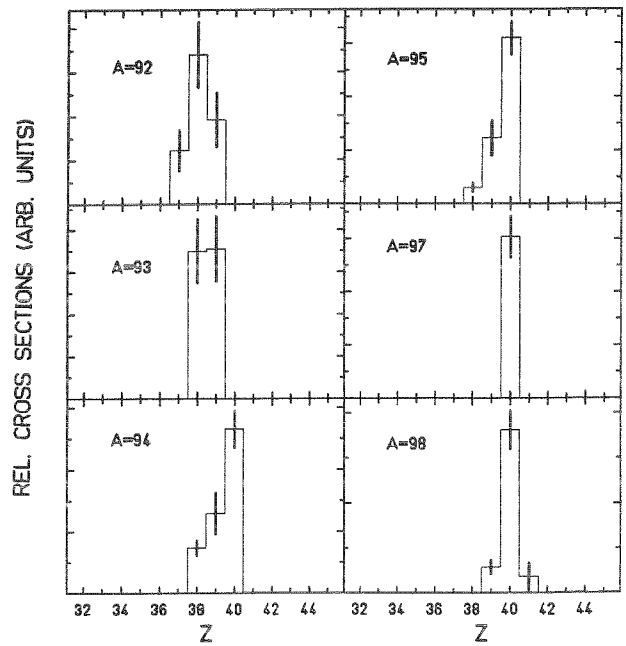

Fig.3: Z distributions in various mass bins for $^{124}Sn + {}^{96}Zr$ at 4.15 MeV/u at 25°(lab).

[1] W.Reisdorf et al., GSI Sci.Rep.1985, p.61

[2] R.Bellwied et al., GSI Sci.Rep.1986, p.46

[3] W.Swiatecki, Nucl.Phys. A376, 275(1982)

[4] C.C.Sahm et al., Z.Phys. A319, 113(1984)

Search for the Formation of Long-Lived Giant Nuclear Molecules in the Collision of Very Heavy Ions [B] Near the Coulomb Barrier.

G. Wirth, W. Brüchle, Fan Wo, and K. Sümmerer
GSI Darmstadt
F. Funke, J.V. Kratz, and N. Trautmann
Institut für Kernchemie, Universität Mainz

Only little is known on the collision dynamics in the reaction of very heavy ions near the Coulomb barrier. The nominal Coulomb barrier $V_C = Z_1Z_2e^2/R_{INT}$ calculated for U + U with the experimentally determined interaction radius of R_{INT} = 16.9 fm is E_{LAB}/A = 6.1 MeV/u. But the ion-ion potential clearly depends on the relative orientation of the two deformed U-nuclei. Several theoretical calculations of the potential including deformation and orientation degrees of freedom were published [1]. Some of these predict shoulders or pockets in the interaction potential which depend on the relative orientation of the deformed actinide nuclei. This could give rise to delayed collisions with deviations from Rutherford trajectories; even the existence of a long-lived dinuclear system was suggested. Nuclear reactions should be influenced by the shape of the potential and may therefore serve as an experimental probe. But using unpolarized beams and targets, the experimental cross sections represent averages over all relative orientations and signatures from only a small fraction of the collisions may be easily hidden. An experimental method to search for the formation of long-lived nuclear molecules, or more generally, a method to search for collisions deviating from Rutherford trajectories therefore must be very sensitive.

Possibly, nucleon transfer might provide a useful experimental tool. Previously, we have shown [2] that for more peripheral collisions the one-neutron transfer probability can be described by a semiclassical sub-Coulomb theory. The transfer probability scales with the distance of closest approach. Deviations from Rutherford trajectories should become visible in the angular distributions of the one-neutron transfer. In the symmetric reaction $^{238}U + ^{238}U$ the experiment cannot distinguish between target-like and beam-like transfer products. The angular distribution for the one-neutron transfer product exhibits a minimum at $\theta_{CM} = 90^0$, and even at energies below the barrier the cross section is high of the order of a few mb/sr. This probably will prohibit the detection of changes in the angular distributions by a small fraction of collisions deviating from Rutherford trajectories. In contrast, a high sensitivity should be obtained in an asymmetric reaction such as $^{238}U + ^{197}Au$. Here, at backward angles, practically no target-like one-neutron transfer products are expected. Fig.1 shows the measured angular distribution of the target-like one-neutron transfer product ^{198}Au from the reaction $^{238}U + ^{197}Au$ at a beam energy below the barrier E_{LAB}/A = 5.6 MeV/u (0.93 * V_C). The expected cross section for ^{198}Au from the semiclassical theory integrated over the angular range $137^0 \leq \theta_{CM} \leq 174^0$ (Fig. 1) is less than 0.01 µb, much lower than the experimental detection limit of ≅ 10 µb. Therefore, the observation of ^{198}Au-products at these backward angles would give evidence for collisions not following Rutherford trajectories.

By now irradiations were performed between 5.4 MeV/u and 6.4 MeV/u at several energies. Data analysis is not yet completed, but at all energies so far no ^{198}Au-activity with a limit of approximately $\sigma \leq 10$ µb was found in the angular range $137^0 \leq \theta_{CM} \leq 174^0$. Under the assumption of an isotropic distribution of the reseparating nuclei after the formation of a long-lived dinuclear system, the cross section limit for the formation of a long-lived dinuclear system with the transfer of one neutron during the lifetime is approximately $\sigma \leq 0.1$ mb in $^{238}U + ^{197}Au$ collisions at the beam energies used so far. If the one-neutron transfer probability in such a long-lived nuclear molecule is not lower than in the corresponding collisions where the nuclei follow Rutherford trajectories, the cross section limit for the formation of a long-lived dinuclear system in a nearly central collision at E_{LAB}/A = 5.9 MeV/u close to the barrier results as $\sigma \leq 0.2$ mb. Further irradiations at various energies will be performed since the search for nuclear resonance scattering of course must be done in small energy steps.

References

1. Rhoades-Brown, M.J., Oberacker, V.E., Seiwert, M., Greiner, W.: Z. Phys. **A310**, 287 (1983)
Seiwert, M., Greiner, W., Oberacker, V.E., Rhoades-Brown, M.J.: Phys. Rev. **C29**, 477 (1984)
Ismail, M., Rashdan, M., Faessler, A., Trefz, M., Mansour, H.M.M.: Z. Phys. **A 323**, 399 (1986)

2. Wirth, G., Brüchle, W., Brügger, M., Wo, Fan, Sümmerer, K., Funke, F., Kratz, J.V., Lerch, M., Trautmann, N.: Phys. Lett. **177B**, 282 (1986)

Fig.1
Angular distribution of the one-neutron transfer product ^{198}Au in the system $^{238}U + ^{197}Au$.

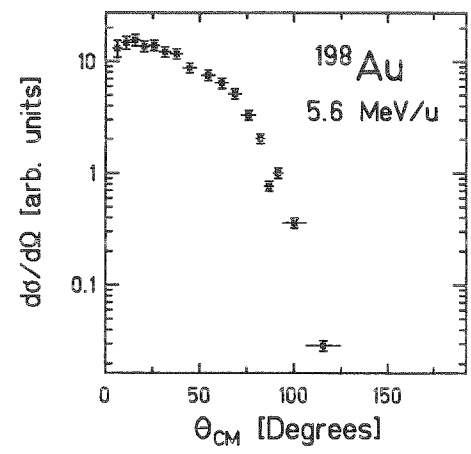

Fission in ^{238}U + ^{238}U Collisions below the Coulomb Barrier [3]

G. Wirth, W. Brüchle, Fan Wo, and K. Sümmerer
GSI Darmstadt
F. Funke, J.V. Kratz, and N. Trautmann
Institut für Kernchemie, Universität Mainz
V.E. Oberacker
Dept. Physics & Astronomy, Vanderbilt University, Nashville, Tenn. 37235, U.S.A

One-neutron transfer is the most probable direct reaction in ^{238}U + ^{238}U collisions at energies below the barrier. Recently we have reported on the excitation function and angular distributions for the one-neutron transfer product ^{239}U[1]. Large deviations from semiclassical expectations, deformation not yet included, were seen for central collisions (Fig.1). But the discrepancies between experiment and calculations are not necessarily evidence for the importance of deformation effects, because sequential fission after transfer could change the angular distributions of the observed surviving 1n transfer product ^{239}U. Then the missing transfer cross section would show up in the fission channel. Therefore, we have measured fission cross sections in U + U collisions at bombarding energies below the Coulomb barrier. Fig.2 tells us that fission is an important reaction channel in U + U collisions below the barrier because quite high cross sections of several mb are measured at low bombarding energies. In principle two processes could lead to fission: Coulomb fission and sequential fission after nucleon transfer. Coulomb fission is well established in the reaction of very heavy nuclei[2] and is essentially a two-step process of multiple Coulomb excitation followed by radioactive decay. We have calculated pure Coulomb fission cross sections (solid line in Fig.2) within a semiquantal theory which already gave satisfactory results in comparison with different Coulomb fission experiments.[2] The exceeding part of the experimental fission cross section over that for Coulomb fission is transfer fission. At all energies up to 6.1 MeV/u, the transfer fission cross sections are much smaller than the observed discrepancies in the corresponding 1n angular distributions. This already answers the main question of the present work: Sequential fission after transfer cannot explain the observed discrepancies in the angular distributions of the one-neutron transfer product ^{239}U. Details are given in Ref. [3]. The same conclusion is obtained by folding calculated angle dependant Coulomb fission probabilities with the experimental angular distribution for the surviving 1n transfer product ^{239}U. The resulting differential cross sections for the sequential fission after 1n transfer are shown as dashed lines in Fig.1. The integrated cross sections reveal that less than 10% of the experimental fission cross sections are due to 1n transfer induced fission.

The experimental fission excitation function increases steeper than the excitation function for Coulomb fission. Fig.2 indicates that in U + U collisions at energies higher than 5.5 ± 0.1 MeV/u transfer induced reactions different from one-neutron transfer become important. This is consistent with the observation of multi-nucleon transfer reactions producing e.g. the 2p9n-transfer product ^{227}Th down to a bombarding energy of 5.6 MeV/u.[4]

1. Wirth, G., Brüchle, W., Brügger, M., Wo, Fan, Sümmerer, K., Funke, F., Kratz, J.V., Lerch, M., Trautmann, N.: Phys. Lett. **177B**, 282 (1986)
2. Oberacker, V.E., Pinkston, W.T., Kruse, H.: Rep. Prog. Phys. **48**, 327 (1985)
3. Wirth, G., et al., GSI 88-01 (1988)
4. Wirth, G., et al., to be published

Fig.1
Angular distributions of the one-neutron transfer product ^{239}U in the system ^{238}U + ^{238}U. The experimental data points and the semiclassical calculations (solid lines) are taken from Ref. [1]. The dashed lines are calculated cross sections for sequential fission of ^{239}U.

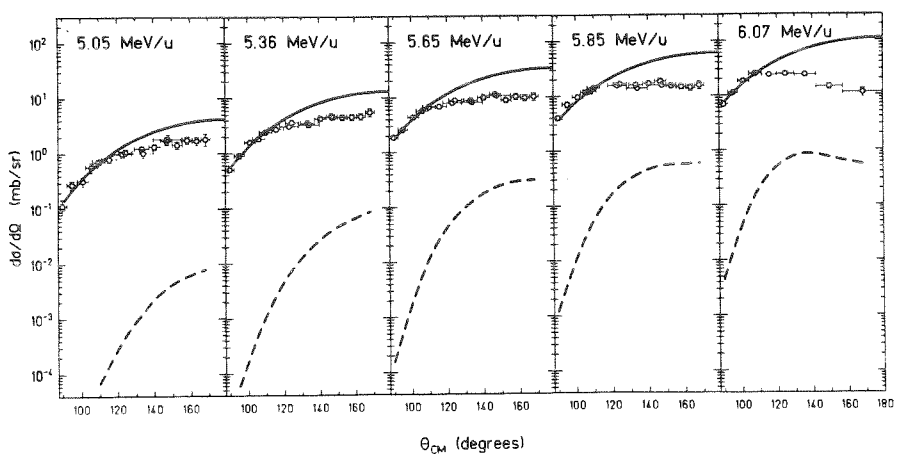

Fig.2
Excitation function for fission in the reaction ^{238}U + ^{238}U. The dashed line is a smooth curve through the experimental data points. The solid line is a calculation for pure Coulomb fission.

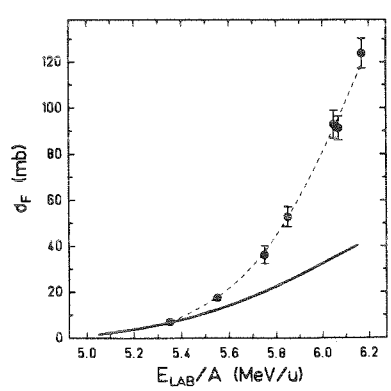

Single and Double Sequential Fission in $^{197}Au \rightarrow ^{197}Au$ at 15 MeV/u

R. Schmoll, Th. Blaich, J.V. Kratz
Institut für Kernchemie, Universität Mainz

K. Sümmerer, G. Wirth
GSI Darmstadt

In preceding experiments [1,2] we have measured the integral $\mathcal{Z},\mathcal{A}$-distribution and the deflection function in the reaction of 15 MeV/u ^{197}Au with ^{197}Au. In an additional, recent experiment, using catcher foil techniques and γ-ray spectroscopy, we have measured two-dimensional angle-velocity distributions for fission fragments. As is shown in Fig.1, these distributions reveal the typical Coulomb hole of sequential fission processes after a first, deep-inelastic reaction step. These are compared with three-body and four-body Coulomb trajectory calculations. In case of the lightest fission fragments, see Fig.1, only four-body trajectory calculations are capable of reproducing the experimental data.

The mass distribution [1] for $24 \leq \mathcal{A} \leq 125$ consists of a narrow (FWHM $\approx$ 25u) peak around $\mathcal{A}$=88 which is superimposed on a very broad distribution (FWHM $\approx$ 110u) around $\mathcal{A}$=83, see Fig.2. Detailed comparisons of experimental two-dimensional angle-velocity distributions for particular fragment masses indicated by the arrows in Fig.2 with Coulomb trajectory calculations reveal that fragments which are part of the broad mass distribution component are formed in a double-sequential break-up of two primary deep-inelastic reaction products. This fission-like process is characterized by an extreme instability with respect to the mass asymmetry coordinate with large probabilities for very asymmetric mass splits like $\mathcal{A}_3/\mathcal{A}_4 = 7:1$, as is the case for the production of ^{24}Na. On the other hand, fragments which are part of the narrower distribution at symmetry are apparently dominantly formed in a single sequential fission of one of the reaction products of the first reaction step. Single sequential break-up is rather narrowly constrained to excitation energies $75 \leq E^* \leq 275$ MeV of the primary gold-like fragments, while the probability for double sequential fission rises steeply above $E^* \approx 200$ MeV and is unity for the highest excitation energies.

The integral cross section of the broad four-body distribution corresponds to 60% of the total reaction cross section; the integral cross section of the narrow three-body distribution corresponds to 10%. These values are consistent with fractional cross sections obtained by folding the primary binary event distribution as a function of the excitation energy (Monte Carlo simulation) with the above mentioned fission probabilities.

The Coulomb trajectory calculations of the two-dimensional angle-velocity distributions and comparisons with experimental data establish a fast time scale for the sequential fission processes such that both the velocities and the angular distributions are modified by a final state Coulomb interaction due to the proximity of the partner system of the first, deep-inelastic reaction step, as reported in Ref. [3].

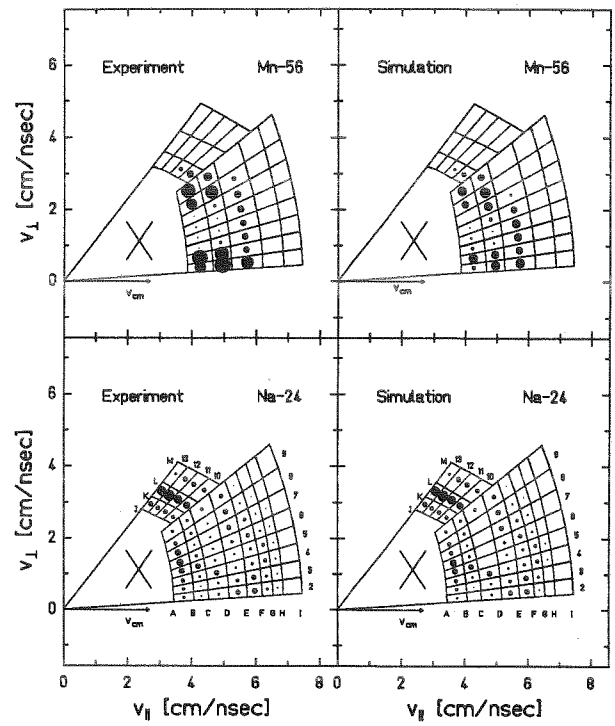

Figure 1: Experimental and simulated angle-velocity distributions for ^{56}Mn and ^{24}Na. The size of the black dots scales with the relative cross sections.

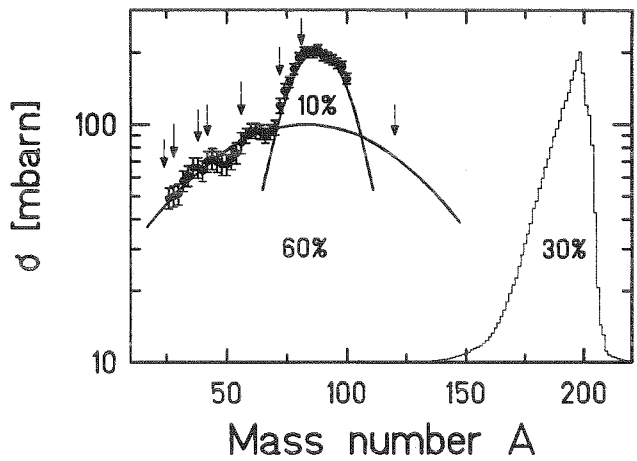

Figure 2: Mass distribution for the system $^{197}Au \rightarrow ^{197}Au$ at 15 MeV/u. The shape of the binary peak was simulated by Monte-Carlo calculations including evaporation. The peak was normalized to 30%. The arrows are indicating mass numbers for which also two-dimensional angle-velocity distributions were measured and calculated.

References

[1] Th. Blaich, doctoral thesis, Inst. für Kernchemie, Universität Mainz, 1987

[2] R. Schmoll et al., GSI Scientific Report 1986, GSI 87-1, p.62(1987)

[3] P. Glässel et al., Z.Phys. A310,189(1983)

Aqueous Chemistry of Element 103, Lawrencium[B]

U.W. Scherer, J.V. Kratz, N. Trautmann, S. Zauner
Institut für Kernchemie, Universität Mainz
M. Schädel, W. Brüchle, B. Schausten
GSI Darmstadt
R. Chasteler, K.E.Gregorich, H.Hall, R.Henderson,
D. Lee, M. Nurmia, D.C. Hoffman
Lawrence Berkeley Laboratory, Berkeley

To investigate the chemical properties of lawrencium, element 103, in aqueous solution we performed two types of experiments:

1. Search for oxidations states lower than 3+
2. Determination of the ionic radius of Lr^{3+}

The isotope 3-min ^{260}Lr and lighter actinides were produced at the Berkeley 88 inch cyclotron in bombardements of a ^{249}Bk target with ^{18}O. Experimental details, and first results were reported earlier.[1,2]

1. We have searched for lower oxidation states in aqueous solutions using Cr^{2+} and V^{2+} metal ions as reductants.[1]. In case of the reduction of Lr^{3+} to lower oxidation states the ions become larger and have obviously less charge. This can be made visible by extraction chromatography with di(2-ethylhexyl)orthophosphoric acid (HDEHP) for which the affinity for metal ions depends sensitively on the size and charge of the ion. The chemical separations did not differentiate between Lr^{2+} and Lr^{1+} ions. Relativistic models predict the monovalent state: The $7s^2$ closed shell acts as an 'inert core' due to strong stabilization by relativistic effects.

In 22 runs we observed 13 events of ^{260}Lr besides large activities of Fermium in the fraction containing trivalent actinides. In the reduced fraction only isotopes of Md were observed, as expected, because Md is known to be reduced to Md^{2+} under these conditions.

From the concentration of the reductants one can estimate an upper limit for the reduction potential with the aid of the Nernst equation. We determined the actual concentration of our reductant (Cr^{2+}) by two independent methods: By reduction experiments with e.g. Eu^{3+}(E_0 = -0.35 V), and spectrophotometrically. The solution contained ≥ 96 % of the chromium ions as Cr^{2+}. This yields an upper limit for the reduction potential of $E_0 \leq$ -0.53 V for the Lr^{3+}/Lr^{1+} half reaction. The reduction experiments with Eu^{3+} defined a Cr^{2+} content of > 55 %. This more conservative estimate yields an upper limit for the reduction potential $E_0 \leq$ -0.44 V.

2. The elution positions of trivalent heavy actinides and lanthanide tracers from cation exchange columns (filled with Aminex A6 resin) were determined by eluting with 0.12 M α-hydroxy-isobutyric acid (pH = 4.85) [2]. We observed 25 decays of ^{260}Lr together with several isotopes of Md and Fm in 93 runs. Fig. 1 shows the elution curves of Lr^{3+} and Md^{3+} together with the lanthanide tracers: Lr elutes together with Er, and Md shortly after Ho. The elution maximum of Lr is not observed in the vicinity of Tm, as expected from simple extrapolations, but much later. The elution position (the distribution coefficient K_D) depends strongly on the ionic radius. Ionic radii can be determined from the correlation of known radii of trivalent lanthanides and actinides to their log K_D values for a fixed coordination number (CN = 6 or CN = 8). These radii can be compared with calculations of the radial expectation values of the core electron wave functions. A plot of such data for CN = 6 vs. the atomic number, see Fig. 2, shows:

1. The slope of the actinide curve is steeper than that of the lanthanide curve. This means the actinide contraction is more pronounced than the lanthanide contraction.

2. The ionic radius of Lr^{3+} is larger than the radius one would obtain by extrapolating the actinide curve. This may be explained [2] by the polarizability of the f-shell electron orbitals which is expected to be more pronounced for the actinides than for the lanthanides, or by a pronounced secondary relativistic effect.

3. Both theoretical predictions describe the lanthanide radii fairly well. The actinide data are in much better agreement with recent multi-dimensional, relativistic Dirac-Fock calculations.[6]

Based on the ionic radii, and by using semi-empirical equations for the determination of the heats of hydration we have obtained

ΔH_{hyd} = - 3654 kJ/mol for Md, and
ΔH_{hyd} = - 3689 kJ/mol for Lr

with an estimated systematic uncertainty of < ± 20 kJ/mol in both cases.

1. U.W.Scherer et al., Preprint GSI-87-68, and Inorg. Chim. Acta in press
2. W.Brüchle et al., Preprint GSI-87-67, and Inorg. Chim. Acta in press
3. J.P.Desclaux et al., J.Physique 41, 943 (1980)
4. R.G.Haire,R.D.Baybarz, J.Inorg.Nucl.Chem. 35, 489 (1973)
5. J.T.Waber, D.T. Cromer, J.Chem.Phys., 42, 4116 (1965)
6. J.P.Desclaux, A.J.Freeman, Atomic Properties of the Actinides, in Handbook on the Physics and Chemistry of the Actinides, p.1, A.J.Freeman and G.H.Lander eds., North Holland, Amsterdam (1984)

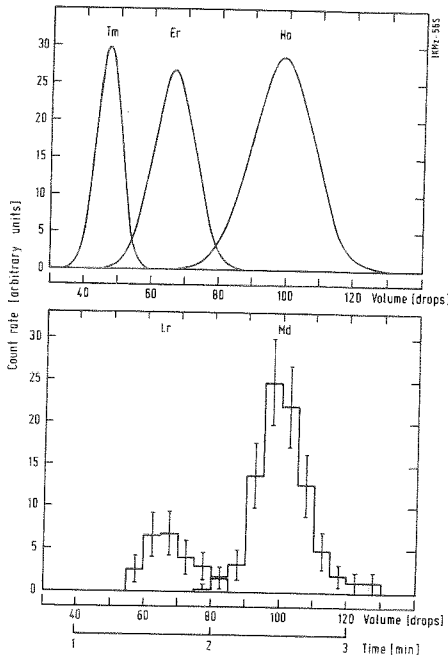

Fig. 1: Elution of Ln^{3+} and An^{3+} ions from CIX columns with α-HIB. The distribution of lanthanide tracers is shown in the upper part, the distribution of Lr^{3+} and Md^{3+} in the lower part.

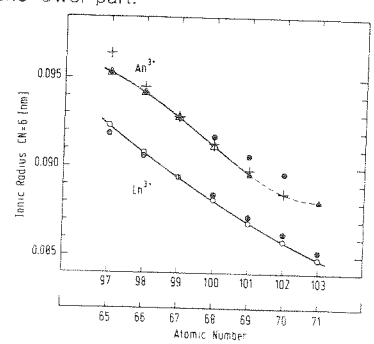

Fig. 2: Ionic radii for CN = 6 of some lanthanides and actinides vs. the atomic number. Our experimental data (full triangles) and data from ref.[4] (open symbols) are compared with results of quantum-mechanical calculations (full points[5], crosses[6]). The lines through experimental data are drawn to guide the eye.

SEARCH FOR LAWRENCIUM AS A P-ELEMENT USING GASCHROMATOGRAPHY TECHNIQUES

D.T.Jost, H.W.Gäggeler
Eidg. Institut für Reaktorforschung, Würenlingen, Switzerland

M.Schädel, E.Jäger
Gesellschaft für Schwerionenforschung, Darmstadt, Fed. Rep. of Germany

B.Eichler, S. Hübener
Zentralinstitut für Kernforschung, Rossendorf, German Dem. Republic

K. E. Gregorich, D.C.Hoffman
Lawrence Berkeley Laboratory, CA94720, Berkeley, USA

Multidimensional relativistic Dirac-Fock calculations[1,2] predict that the last member of the actinides series, Lr, might behave like a p-element with a [Rn] $5f^{14}$ $7s^2$ $7p_{1/2}$, Lr(p), ground state electronic configuration, rather than the traditionally expected [Rn] $5f^{14}$ 6d $7s^2$, Lr(d), configuration.

Extrapolating the adsorption enthalpy for Lr(p) on quartz from the known values of the group III elements Al, Ga, In, Tl gives a value of 94±9 kJ/mol. Model calculations of the partial molar adsorption enthalpy of a gaseous metal on a metal surface at zero coverage give an adsorption enthalpy for Lr(p) on Pt of 187 kJ/mol and for Lr(d) of 749 kJ/mol[3].

^{260}Lr with a half-life of 3 min, produced in the reaction of 101 MeV ^{18}O + ^{249}Bk at the 88" cyclotron at the LBL, with a cross section of 8.3±1.7 nb[4], was used for these experiments. It decays by α-emission with E_α = 8.03 MeV[5]. A gas-jet coupled to a high temperature gaschromatograph and subsequent reclustering was used to transport the activities to the rotating catcher wheel (MG-wheel)[6].

The first part of Fig. 1 (labeled "DIRECT CATCH") shows the integral α-spectrum from an experiment without chemistry. The main α-peaks are due to the decay of 250-254Fm, ^{249}Cf, ^{211}Bi and ^{210,211}Fr. The small α-activity between 7.97 and 8.06 MeV are attributed to ^{260}Lr. This activity corresponds to a production cross section of 9.6±1.6 nb which is in good agreement with the value of 8.3±1.7 nb[4]. This assignment is further corroborated by a decay analysis of this event group giving a value of 2.3±1.0 min.

The second part of Fig. 1 shows the result of the gas phase chromatography experiment in which the quartz chromatography column was used at about 1000 °C. As expected, the Fm isotopes are adsorbed on the quartz column at this temperature and do not appear in the spectrum in contrast to the 6p-element Bi. The ^{249}Cf peak is due to a minor contamination of the counting device from a previous experiment.

The third part of Fig. 1 shows the spectrum obtained with a Pt chromatography column at about 1000 °C. Here ^{211}Bi too is retained in the column and hence no activities other than the ^{249}Cf contamination were observed.

In neither the quartz- nor the Pt-experiment any ^{260}Lr events could be detected. If Lr would have been volatile 20 respectively 15 events should have been seen. These values can be converted to a lower limit of the retention time of about 7.5 min at a 95% confidence level which in turn gives a lower limit for the adsorption enthalpy for Lr on both surfaces of $-\Delta H_a \geq 290$ kJ/mol. This value is significantly higher than the expected values for Lr(p) on quartz and Pt.

Therefore the existence of the [Rn] $5f^{14}$ $7s^2$ $7p_{1/2}$ electronic structure for the ground state of Lr could not be confirmed by our gas chromatography experiments. These experiments, however, also do not disprove the existence of Lr(p). Since the ground state energy of Lr(d) is only 93 kJ/mol higher[2] than that of Lr(p) the column surface could cause Lr(p) to be promoted to Lr(d) in the adsorption process.

1. J.P. Desclaux, et al., J. Physique 41, 943 2. (1980)
2. L. Brewer, High Temp. Sci., 17, 1 (1984)
3. B. Eichler, et al., Inorg. Chim. Acta, in print
4. D. C. Hoffman, et al., Proc. Conf. on Methods and Applications of Radioanalytical Chemistry, Kona, Hawaii, April 1987, J. Radioanalyt. Chem. in print.
5. K. Eskola, et al., Phys. Rev., C4, 632 (1971)
6. D. T. Jost, et al., Inorg. Chim. Acta, in print.
7. B. Eichler, Report ZfK-396, Zentralinstitut für Kernforschung, Rossendorf (1979)

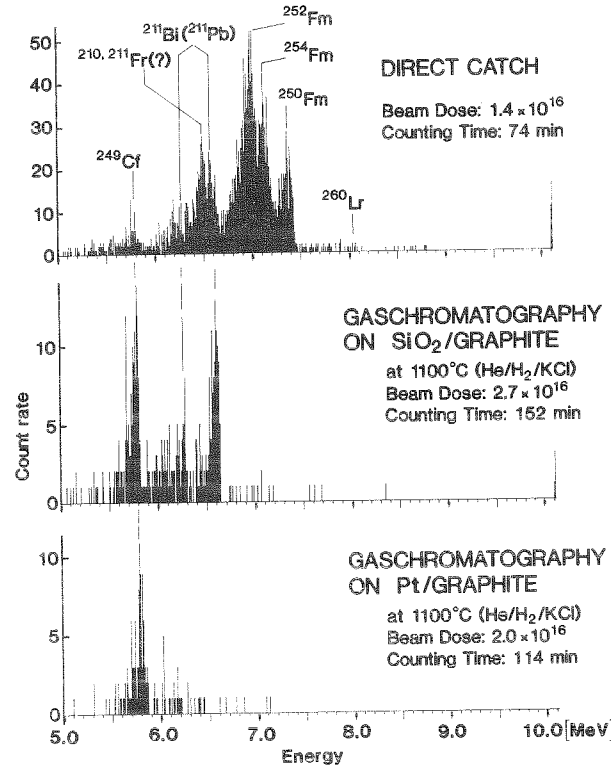

Fig. 1: Integral α-spectra from detector 2 top (covering the time from 2 to 4 min after the end of the deposition) for the three experiments: 'DIRECT CATCH': no chemistry, 'SiO2/GRAPHITE': separation in a quartz column at about 1000 °C, and 'Pt/GRAPHITE': same as above with a platinum column.

A Scheme for the chemical Separation of all Elements between Gold and the Lanthanides

W. Brüchle, M. Schädel, B. Schausten, B. Szweryn
GSI Darmstadt

It has been found that above a total incident energy of 3GeV the region of "limiting fragmentation" is reached in which the cross sections for proton- and light-ion induced spallation products differ only by the ratio of the total geometric cross sections. A parametrization for a general description of the isotopic yields based on the experimentally available data for lighter elements up to A ~ 100 has been made by K. Sümmerer [1]. To check the validity of his formula up into the region A ~ 200, and thus enable predictions for the production rates of such heavy exotic nuclei at the fragment separator, a reliable data base of experimentally determined spallation cross sections in this mass region is badly needed.

We want to separate the elements Lu, Hf, Ta, W, Re, Os, Ir, Pt, Au, and Tl after irradiations of gold targets with 3GeV protons at the "Laboratoire National Saturne", Saclay. Independant cross sections for individual isotopes with half- lives of about 1 hour and longer can be determined after the observation of characteristic γ-radiation. To enhance the sensitivity for neutron- rich isotopes which are produced with low cross sections of about 1μb we will use a β^--γ- coincidence which suppresses the intense background of EC- decays.

The following separation scheme was worked out:

After dissolving the gold target or catcher foils in aqua regia, Os is distilled as OsO_4 and extracted into chloroform. Some percentage of Re is volatile as Re_2O_7 which is not extracted but later on transferred to the Re preparation. After backextraction with NaOH Os is precipitated as a sulfide. Au^{3+} and Tl^{3+} are extracted with diethylether. To prepare a sample Au is reduced to the metal by SO_2, Tl is precipitated as TlJ. After adding hydrofluoric acid we extract Ta and Re in di-isopropyl-ketone. Both elements are backextracted in water. Re can then be extracted into methyl- ethyl- ketone, whereas Ta is coprecipitated with an iron hydroxide scavanger. The solution which contains all other unseparated ions will be boiled to dryness with boric acid to remove hydrofluoric acid. The next separation is performed by a cationic exchange (CIX) procedure. The first fraction contains W and the platinum metals. WO_3 can be precipitated after addition of some carrier from a concentrated nitric acid solution. Pt and Ir are separated by use of a anionic exchange. Most of the Ir^{3+} elutes with HCl; some percentage of Ir^{4+} is washed out with KOH. Pt is then eluted with $HClO_4$. The final samples are made by a sulfide precipitation. The next fraction from the CIX column contains only contaminants which are discarded. The third fraction with dilute HF contains Hf which is further cleaned by an extraction into tributylphosphate. The last fraction yields the rare earth elements. They are separated from each other on a second CIX colum which is eluted with α-hydroxiisobutyric acid.

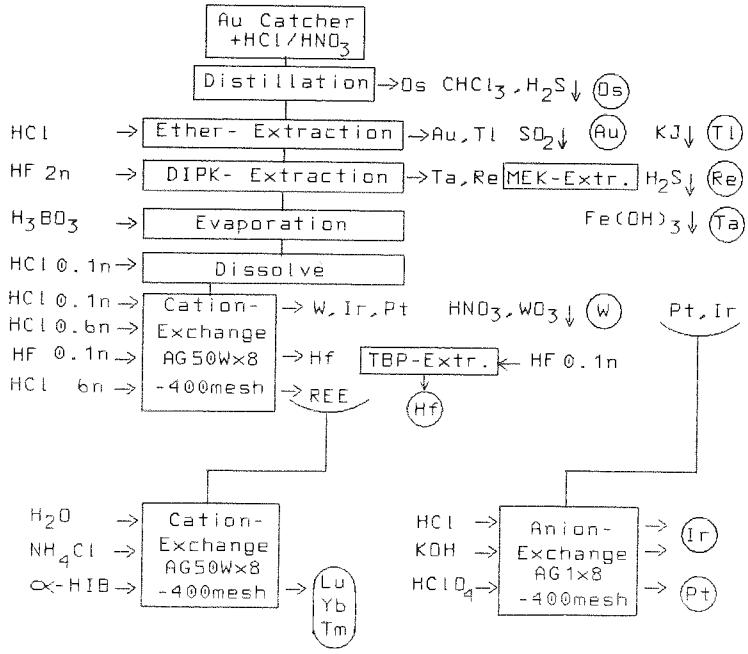

1 K. Sümmerer, GSI Scientific Report 1986, GSI 87-1, 97

A Detector System for the Search of Exotic Nuclei via Rutherford Backscattering [B]

A.Breskin[1], R.Checik[1], Z.Fraenkel[1], G.Herrmann[2], K.Lützenkirchen[3], M.Overbeck[2], S.Polikanov[3], N.Trautmann[2] and Th.Wilpert[4]

[1]Weizmann Institute, Rehovot, Israel

[2]Institut für Kernchemie, Universität Mainz

[3]GSI, Darmstadt

[4]Hahn - Meitner Institut, Berlin

A detector system has been built, designed for the search of exotic heavy nuclei /1/ by means of Rutherford Backscattering. A heavy-ion beam, preferably ^{238}U or ^{208}Pb, of energy 1.4 MeV/u impinges on a target prepared from natural samples. A possible content of heavy particles (mass $\geq 10^3$GeV) should result in backscattered projectile particles. The quantities that need to be measured in order to classify a scattering event are the particle's velocity, scattering angle and specific energy loss. This requires the use of a START- and a STOP-detector which both have to be position-sensitive in order to perform a track-reconstruction of the event. Since the ions to be detected are quite slow ($E/A \leq 1$ MeV/u) both detectors have to be thin.

These requirements can be met by Multi-Wire-Proportional-Chambers (MWPC) operating at low gas pressure /2/. The complete system, installed in GSI's Stripper Hall, consists of 4 START-detectors and 8 STOP-detectors (see Fig.1). It covers the backward hemisphere of the target with a solid angle of 1.5 str. The START-detectors are placed in a semi-circle at 20 cm distance from the target. Two rows of 4 STOP-detectors each, one on top of the other, form a second semi-circle at 65 cm from the target.

The START-detector has an active region of 9•21 cm². Its central electrode is a wire-anode, from which the time signal is taken (see Fig.2). The anode is stacked between two cathodes which are at 90° degrees one with respect to the other for position read-out. The anode plane, made of 10 µm diameter wires, 1 mm apart, is subdivided into 2 timing sections to reduce capacitance effects. Cathode planes are made of 50 µm diameter wires, 1 mm apart. Groups of 3 wires are connected to tapped delay-lines (2 ns/tap) to provide position information. The frames are assembled with pins and screws traversing the frames. The gas tightness is guaranteed by rubber O-rings embedded in the frames, and by two thin gas windows. The window foils are made of 100 µg/cm² polypropylene. They are coated on the inner side with 35 µg/cm² silver to obtain a better RF-shielding of the detector and to connect the foil to ground potential.

The STOP-detector (see Fig.2) is a 28•28 cm² MWPC similar to the START-detector. Its anode is divided into 4 sections, groups of 4 wires are connected to delay-line taps, and the window thickness is 210 µg/cm² Mylar. The STOP-detector has an additional and independent conversion drift space, 20 mm long, coupled to a PPAC stage for measuring the specific energy loss. The PPAC planes are made of 50 µm wires, 1 mm apart.

In order to obtain a time signal of small width both cathodes are put on a potential of -80 V. Otherwise electrons created outside the volume defined by the two cathodes would diffuse into the amplification region and produce a 100 ns tail of the time signal. The usual potential applied to the anode is 420 V.

The time resolution (fwhm) for both counters was measured with 120 MeV ^{58}Ni-ions on a 100 µg/cm² Au-target and a pressure of 2.2 Torr isobutane. A 50 mm² surface barrier detector was fixed just behind the MWPC. The resolutions were found to be 350 ps for the START- and 270 ps for the STOP-counter.

The resolution of the specific energy loss was measured under the same conditions, and was found to be 12%. The voltage in the drift region was 40 V/cm•Torr, and in the parallel plate region 440 V/cm•Torr.

The position of the avalanche on each of the two coordinates is obtained by measuring the time difference of the induced pulses propagating towards the two ends of each delay-line. Position resolution was measured at 2.2 Torr of isobutane with ^{252}Cf fission fragments. A collimator of 300 µm slits was placed at a distance of 15 mm from the entrance cathode, and the ^{252}Cf source was fixed at 40 cm distance from the slit array. The measured resolutions for the START- and STOP-counter are 0.5 mm and 1.6 mm.

/1/ K.Lützenkirchen et al., GSI Annual Report 1986
/2/ A.Breskin et al., Nucl.Instr.Meth.217 (1983) 107

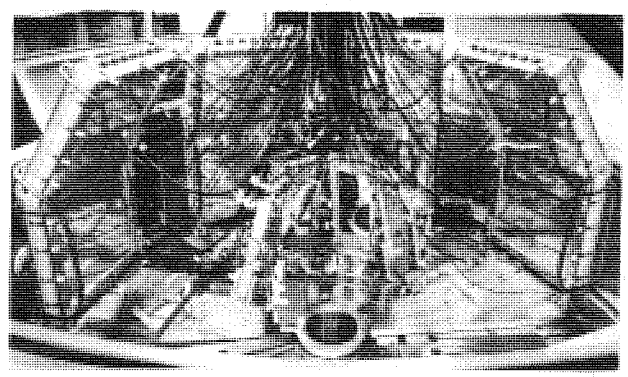

Fig.1: The detection system

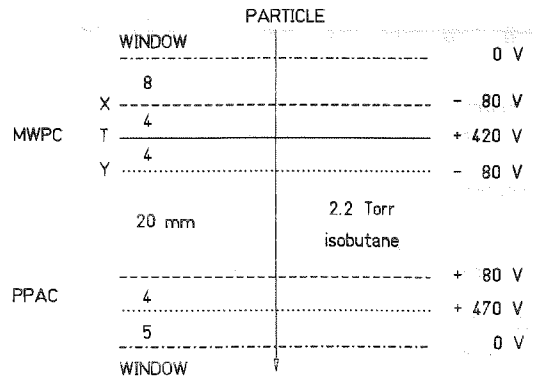

Fig.2: Schematic view of the STOP-detector

Detailed Analysis of the UNILAC U-beam

H. Bokemeyer, D. Schüll, L. Dahl, J. Klabunde, A. Nicklas, P. Strehl,
D. Wilms, G. Wirth, A. Ziem (GSI, Darmstadt);
T. Cowan, J.S. Greenberg, S. Henderson (Yale Univ., New Haven);
K. Bethge, D Kraft, P. Salabura, K Sakaguchi, K.S. Stiebing (Univ. Frankfurt);
B. Kohlmeyer, (Univ. Marburg) D. Schwalm (Univ. Heidelberg)

Investigations of the isoenergetic electron positron emission with the EPOS spectrometer (Z2) /1/ launched the speculations, that contaminations in the U and Th beam could exist. An occasional appearance of these might be correlated with variations observed for the intensities of the positron lines. These considerations were supported from the observation of satellite lines in the spectra of the surface barrier detectors of beam diagnostic facilities, not fully explained by detector defects.

The measurements /2/ were performed with a usual set of U sources with the machine adjusted for ^{238}U beam with an energy of 5.9 MeV/u. This setting then was kept constant during the whole experiment including the calibration measurements with Sn and Mo sources. The beam quality was controled at several stages along the accelerator and the beam transport line. These checks include measurements at the mass analysing system of the injection, the X-ray spectrometer in the stripper section and the surface-barrier detectors (T15 and Z2). A detailed beam analysis was finally performed using the magnetic spectrometer in Z1. For the occurance of a contamination it was assumed that this has to be present already in the 'mass spectrum' produced by the source at the injection slits. The probability of any additional contamination produced at later stages of the accelerator is considered to be negligable small.

As a result, the UNILAC beam proved to be extremely clean at a level of 10^{-4} or better; the only contaminations found are the isotopes ^{94}Mo and ^{94}Zr. Because of the geometrical structure of the accelerator only ions having the same local velocity value at all stages of the machine are accepted. Thus only isotopes which match the specific charge ζ/A of ^{238}U are accelerated to the same specific energy (MeV/u) and velocity and pass the beam transport line if not newly stripped. The change of ζ/A depends characteristically on the individual element. Consequently most of the contaminations which passed the injection slits because of an accidental degeneracy in ζ/A are rigorously eliminated at the stripper section. This is the case for all W isotopes and for ^{235}U observed in the injection 'mass spectrum'.

Only the isotope ^{120}Sn within the resolution of the magnetic system appears to be degenerate with ^{238}U in all sections of the machine, but no ^{120}Sn contamination was found in the source spectrum nor in the analyzed beam. Only contaminations of the isotopes ^{94}Mo and ^{94}Zr have been identified with the magnetic spectrometer. In fact, leaving the stripper section with the subequilibrium charge state 11^+ these isotopes are again degenerate with ^{238}U. They survive the magnetic selection in both the stripper and the beam transport and remain as weak contaminations at nearly half the total energy of U. Unfortunately, the U sources happen to be operated with thermal shieldings made from Mo. Thus contaminations of at most 5×10^{-4} can be present in cases of moderately adjusted injection slits as it is typical for the operation of ^{238}U beams. Higher relative intensities appear to be very unlikely. Only when probing the very unfavourable coincidence of misoperations of both the source and the stripper, with the source at wrong sputter conditions and the stripper at a reduced gas pressure, increased relative Mo intensities of $\leq 3 \times 10^{-2}$ have been reached. The origin of ^{94}Zr, which was found to be less intense by about a factor of 3 (i.e. $< 2 \times 10^{-4}$) could not be clarified.

It was interesting to realize that an occasional weak intensity distribution in the neighbourhood of the ^{238}U mass peak in the source spectrum at higher masses (roughly corresponding to ^{239}Pu) was identified as the isotope ^{238}U itself. The shift is supposed to be caused from an increased local potential within the source due to the sputter voltage; no ^{239}Pu contamination was found in a neutron activation analysis performed from the source material. Finally, the aspect of energy satellite lines in the beam spectrum was studied by a close examination of the time-of-flight spectrum obtained with the particle spectrometer (Z1). Energy satellites found (besides the Mo and Zr contaminations) differ from the main energy by few ‰ only and are assumed to correspond to different regions in the phase ellipsoid differently optimized by operational conditions.

The weak contaminations of the U beam observed in this search can not be correlated with the appearance of the positron lines. Both Mo and Zr clearly differ in the scattering pattern from the U like scattering events obtained in kinematic coincidence measurements as rigorously performed in the EPOS experiments. The event pattern also differs in the unprobable case that Mo or Zr contaminations are additionally present in the target, then leading to fission events. Furthermore, no narrow line structures have been found in a subsequent test run with the EPOS spectrometer (Z2) which could be associated with Mo collisions. For these studies an intense Mo beam was obtained by using a Mo instead of the U source, but leaving the UNILAC and beam transport at essentially identical conditions.

/1/ T. Cowan et al., Phys. Rev. Lett. 56 (1986)444
/2/ H. Bokemeyer et al., Internal Rep., GSI, Darmstadt(1987), GSI-UNILAC-INT/87-3